JOURNAL OF MATERIALS SCIENCE **35** (2000) 3989–3995

Deformation created by the impact of small angular and spherical particles on individual grains

M DUNDAR, O. KELES, O. T. INAL
New Mexico Institute of Mining and Technology, Department of Metallurgical and Materials Engineering, Socorro, NM, USA
E-mail: inal@nmt.edu

Damage mechanism induced by 25 μm, average size, angular and spherical particles impacting the surface of Cu-30% Zn (α-brass) was investigated. Particles were impacted to the surface at normal incidence, with a velocity of 12 m/s. The primary characterization tools used were scanning electron microscopy (SEM) and atomic force microscopy (AFM). AFM allowed for the measurement of impact profiles, those of the cut surface and material pile-ups. Deformed volume by the particles was limited to a single grain. The impacts produced were asymmetrical and the chip formation was also highly directional. These asymmetries were the same in a single grain but they varied from grain to grain. Regardless of particle geometry, similar deformation features were observed on the target surface impacted by angular and spherical particles. The direction of the deformation appeared to be imposed by the mechanical response of the deforming grain. Since the deformation induced by a single impact is limited to a single grain, anisotropic mechanical properties of the individual grains observed were attributed to their impact damage morphology.

1. Introduction

Characterization of erosion caused by solid particles has been extensively investigated for medium (75 μm) and large (500 μm) particles impacting to the surfaces at relatively high velocities [1–6]. Steady state erosion rate is usually the only criterion used for the comparison of resistance of different materials. Assessments that relate the macroscopic mechanical properties of polycrystalline target materials, such as yield strength, fracture strain, fracture toughness and hardness to their erosion resistance can not be satisfactorily generalized to wide range of materials [7–11]. In addition, solid particle erosion caused by the particles smaller than 30 μm and associated deformation mechanism have not been established. Details of these experiments reveal that any proportion, in terms of size between deforming and deformed bodies, were not established either. Relative grain size of target material with respect to the size of impacting particle has not been taken into consideration, thus, rather than deformation of a representative volume, that is an individual grain, deformation of the whole polycrystalline medium and its associated mechanical properties form the major data in terms of anticipated mechanical response of the target material. Accordingly, observed deformation mechanism induced by large particles, is extrapolated to the whole particle size range. Since it is quite certain that deforming volume by the impact of small particles is limited to an individual grain, the mechanical response of an individual grain or, in other words, a "single crystal" should determine the deformation characteristics of single impact.

Preliminary results of the present study exhibit highly directional material flow at the single impact sites of angular particles within the same grain. This asymmetrical material flow is seen to vary from grain to grain. Anisotropic mechanical behavior of a single crystal, accordingly its crystallographic orientation, was related to these observations. Furthermore, one could postulate the influence of angularity of particles as the primary reason of these unusual observations. For this reason, in the present work, spherical particles having same average size, to those of angular particles, were used to elucidate the contribution of crystallographic orientation on deformation mechanism of single impact by suppressing the angularity of the particles.

2. Experimental procedure

Surface of a FCC material, Cu-30% Zn (α-brass), was exposed to the impact of angular SiO_2 and spherical sodalime particles. Average particle size of these erodents was 25 μm (Figs 1 and 2). Since physical properties of soda-lime are close to those of natural silica particles, these were preferred to be used as the spherical particles [12]. Velocity of the particles was 12 m/s and impacted the surface at normal incidence. Since the system delivering the particles to the target is operated in

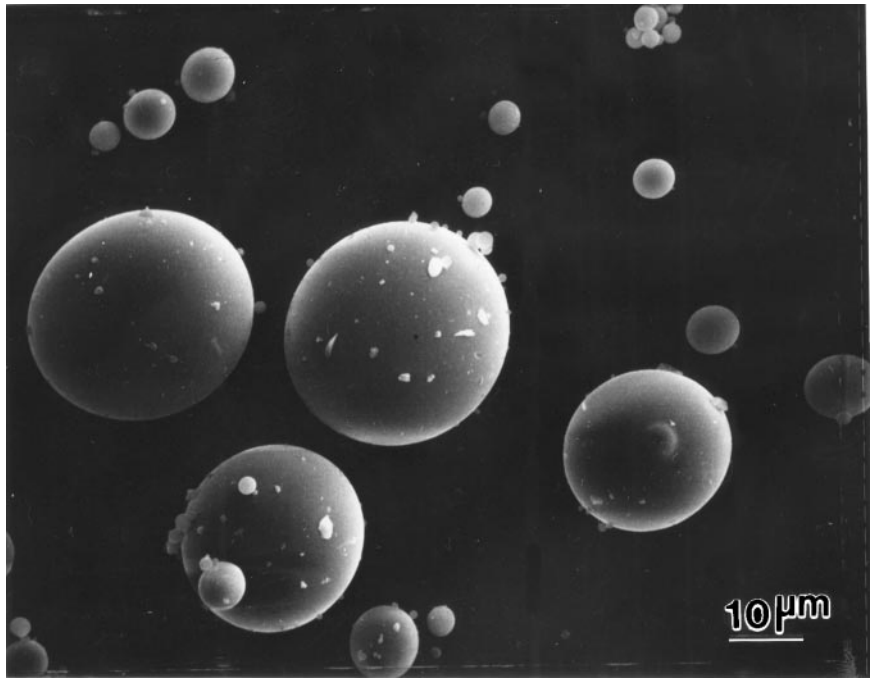

Figure 1 SEM micrograph of 25 μm spherical soda lime.

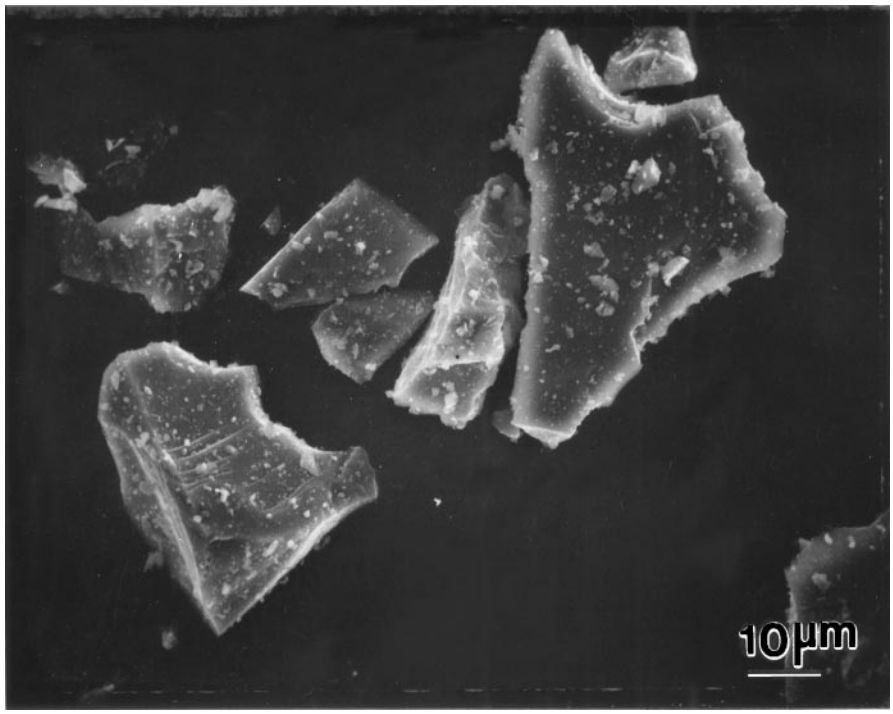

Figure 2 SEM micrograph of 25 μm angular particles.

vacuum, uncertainties regarding impact angle and velocity are eliminated. Prior to the erosion test, samples were electropolished to obtain perfectly smooth and relatively stress free surfaces. This also allowed us to observe very intricate details of the deformation features at single impact sites. Small amount of charge (16 g) impacted to the surface prevented overlapping of more than one indent. In addition to the impact of angular and spherical particles to different target materials, another charge prepared by blending equal amounts of spherical and angular particles was impacted to the surface of the target. Operation of the experimental apparatus and other experimental details are described elsewhere [12–14].

Scanning electron microscopy (SEM) and atomic force microscopy (AFM) were used to document the deformation characteristics of single impact sites. Quantitative analysis was conducted with the help of AFM.

3. Results

Samples were ultrasonically cleaned after the test. Impact sites did not exhibit any sign of particle agglomeration. Figs 3 and 4 show the surface impacted by

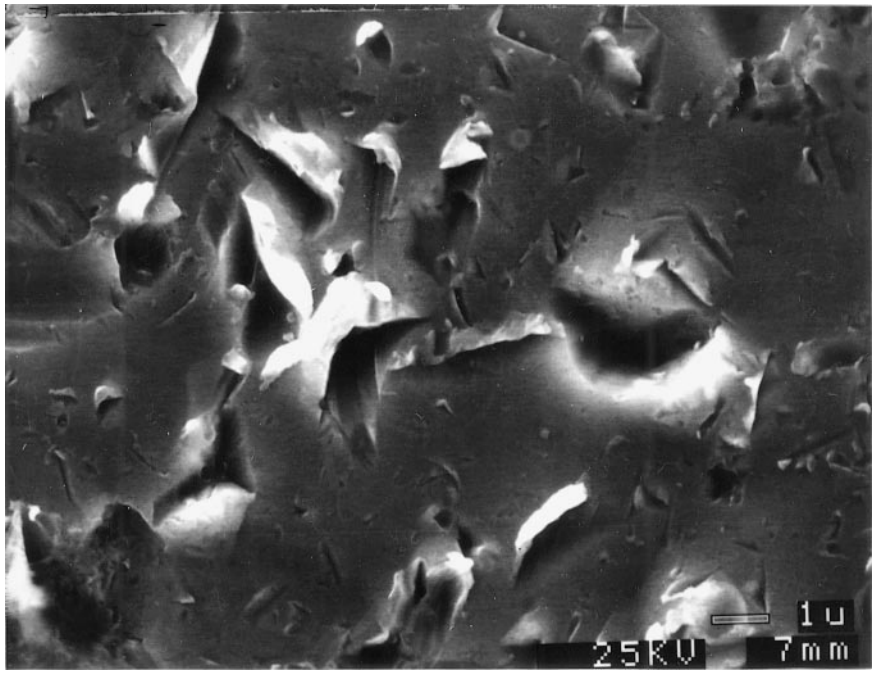

Figure 3 Indentation created by 25 μm angular particles on the surface of individual grain.

Figure 4 Another arbitrarily chosen grain impacted by 25 μm angular particles. Note the identical of chip formation for large and small impacts.

25 μm angular silica particles. Although the impact angle was 90°, displacement of material at the surface was in the form of chips formed by the cutting action of the particles. Both figures show arbitrarily chosen grains impacted by the particles. Due to the large grain size (about 200–250 μm) compared to an individual indent size, any deformation constraint associated with deformation of the grain boundaries was not possible, unless indents occurred at the immediate vicinity of the grain boundary. Asymmetrical material pile-up and direction of cut surface are the same. These two Figs 3 and 4, constitute the best examples for the preferential cutting of the surface in certain directions. Asymmetrical material pile-up and direction of cut surface are the same for the impacts within the same grain. Especially in Fig. 3, traces of cutting action and inclination of newly formed cut-surface and dominant mechanism for the deformation are very typical. Remarkable chip formation and resultant loosely attached material in front of the displacement direction, are common features observed. In Fig. 4, two indents, apparently created by particles at different size, exhibit identical features to that of previous micrograph. Both particles cut the surface by following a curved path in counterclockwise direction. Same deformation mechanism appears to be operative, but in clockwise direction, for the indents in Fig. 3. Directionality in cutting action in different grains and its relationship with the crystallographic orientation of the

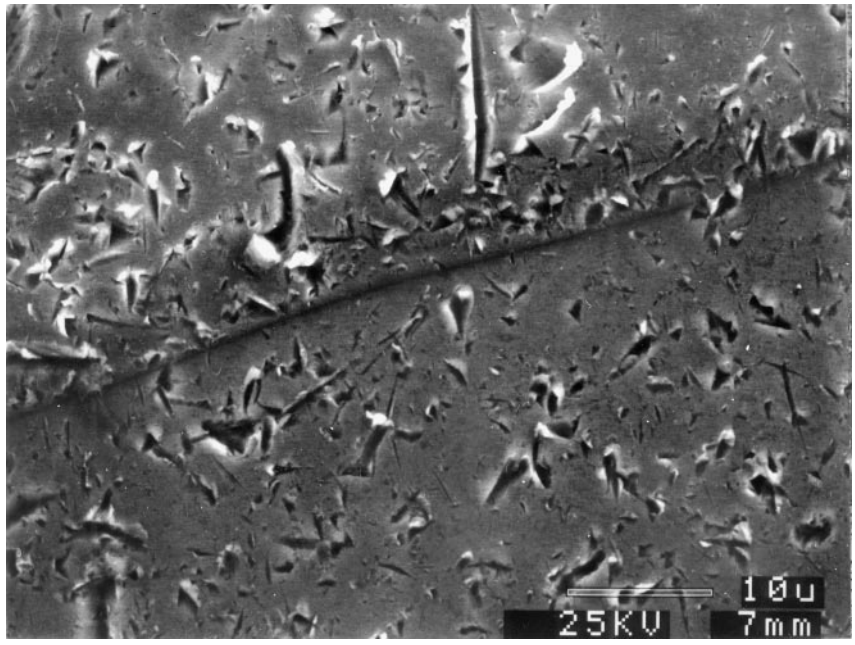

Figure 5 Two neighboring grains are shown. Differences in deformation of individual impact can be easily identified.

grain necessitates investigation with the help of other, more, elaborate, SEM techniques.

Indent size of single impacts, limited to a single grain, offers a possibility of observing deformation characteristics for grains having different crystallographic orientations. Further assessments of this subject will be made in the discussion section and support for this hypothesis comes from a representative area showing two neighboring grains in Fig. 5. Channeling contrast differences between the two grains suggest that they have different crystallographic orientations. It can be assumed that each grain was exposed to approximately the same number of impacts. There are differences between the two grains in the frequency of material pile-ups, the directionality of cutting action, and the amount of material piled-up. Material pile-ups are more extensive in the upper grain. Notice that there is hardly any protrusion of material around the rims of the crater in the lower grain.

Although SEM studies were conducted at very high magnifications (10–25 kX) slip traces could not be observed in the immediate vicinity of indents. Tilting the specimens did not reveal any slip traces around the indents either.

To date, topographic 3-D analysis of the impacted or eroded surfaces are not available in the literature. The chaotic nature of heavily eroded surfaces do not exhibit distinctive features from each other in steady state erosion; these could not provide satisfactory images to elucidate a deformation mechanism for solid particle erosion. AFM imaging was thus limited to samples with a few impacts in the present study. Detailed AFM analysis of single impact sites and surrounding areas of craters were presented in other studies by the authors [15, 16]. Craters were quantitatively characterized by measuring the depths and heights of pile-ups formed at the rims. Fig. 6 shows scanned area and three-selected crater profiles on a sample impacted by 25 μm angular particles. Directions of measurements are drawn on the figure. Inclination of the crater walls at the pile-up and opposite (cutting) side is very similar for the craters. Depth and pile-up heights from different craters are very close in magnitude for this particle size. If the displaced total volume forms the chip, this is an expected observation. Highly directional material flow around the indents can be observed in Fig. 7. Scanned areas around the indentations did not reveal any slip traces.

Three craters, in Fig. 8, were produced by the impact of 25 μm spheres. Impact angle was 90°. Although the craters are not as sharp as those created by angular particles, very clear asymmetric material pile-ups exist at the rims of all craters. Pile-ups are located at the south and east sides of the craters. Fig. 9 shows another randomly selected grain and indentations created by 25 μm spherical particles. Shiny regions of the crater rims suggest that material is displaced above the surface plane. Indentations are not perfectly circular; they are distorted in the direction of pile-ups, note the location of material protrusion at different sides of crater rims in Figs 8 and 9. In contrast to those of the 25 μm angular particles, slip traces were detected around the indentations.

Fig. 10a and b show target surfaces impacted by the mixture of spherical and angular particles. Micrographs show indentations on individual grains. Directionality in chip formation is the same for the individual impact sites of spherical and angular particles. Regardless of particle geometry, asymmetry in material flow is in the same direction.

4. Discussion

It is impossible to predict the first point or area of an angular particle contacting with the target surface. Irregular geometry and accordingly the rotation of the particle make this situation quite unpredictable. Thus, individual impacts can be considered as an event that

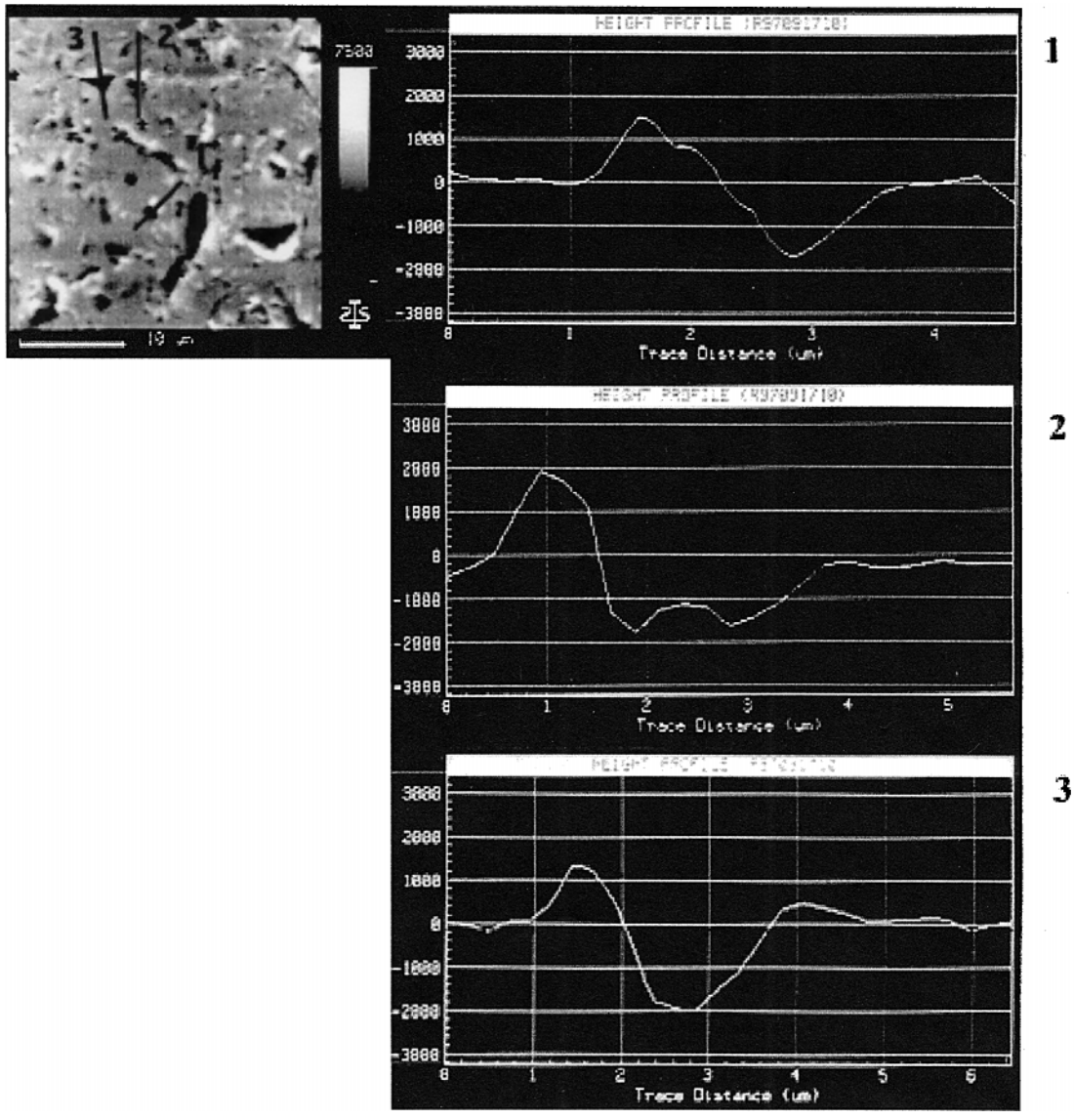

Figure 6 SEM image from selected area. Surface was impacted by 25 μm angular particles. Three crater profiles are shown.

is statistically independent from the previous or future impacts. Therefore, reproducibility of similar deformation features that are the consequence of two different events occurring at different times appear to be a distant possibility in this particular case. However, there are two results common to almost all of these statistically independent events of impacting angular particles; directionality of the material pile-up and the direction of the surface-cut.

One argument to explain directionality in pile-up formation could be based on the angularity of the particles. Asymmetrical geometry of an impacting angular particle can not impose similar loading conditions that of an object having axisymmetric geometry (i.e. spherical particle) on a deforming body. Inclination of cut surfaces, their directionality and crater depth and pile-up height measurements obtained through AFM studies suggest that deformation characteristics of single particle impact is extensively controlled by crystallography of impacted grain. This result is more pronounced for the adjacent craters formed by spherical particles within the same grain, even in the absence of oblique impact. The asymmetrical protrusion, at the rim of the circular craters, undoubtedly lead to the same conclusion. That is, after hitting the surface, path imposed to the particle during penetration is determined by the mechanical response of the deforming grain. If there is a potential influence of particle angularity on the deformation mechanism, this should be obviated by the choice of spherical particles. A spherical particle is symmetrically in contact with the deforming material, but asymmetrical deformation features were observed in this case as well. If there exists an anisotropy in mechanical properties of the deforming material, this would exhibit itself in the form of asymmetrical material protrusion at the rim of the craters. Regardless of the geometry of the particles this was observed for both geometries (i.e spherical and angular). Due to the relative size of the deformed volume, compared to the grain size, mechanical response of the deforming material is identical to that of a single crystal under load induced by the particle. Any constraint on the deforming grain, for example, as might be imposed by grain boundaries, is very unlikely in the present study, unless impact occurred at the immediate vicinity of the grain boundary as indicated earlier.

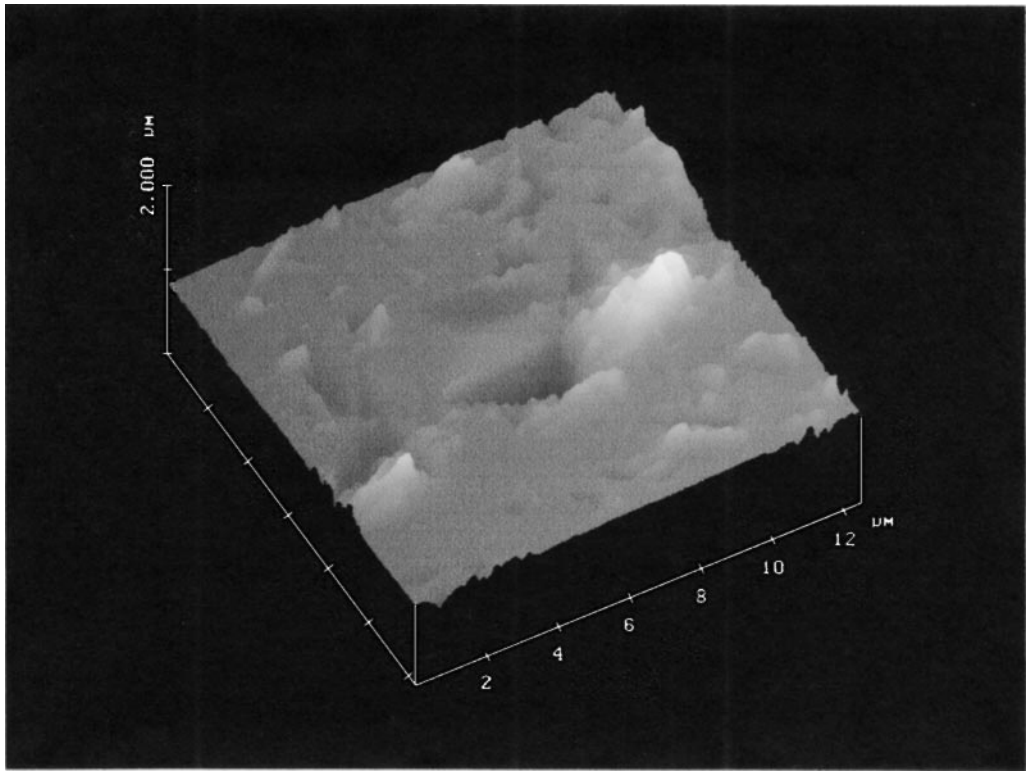

Figure 7 3-D image of a surface impacted by 25 μm angular particles. Note the directionality of material flow around the indentations.

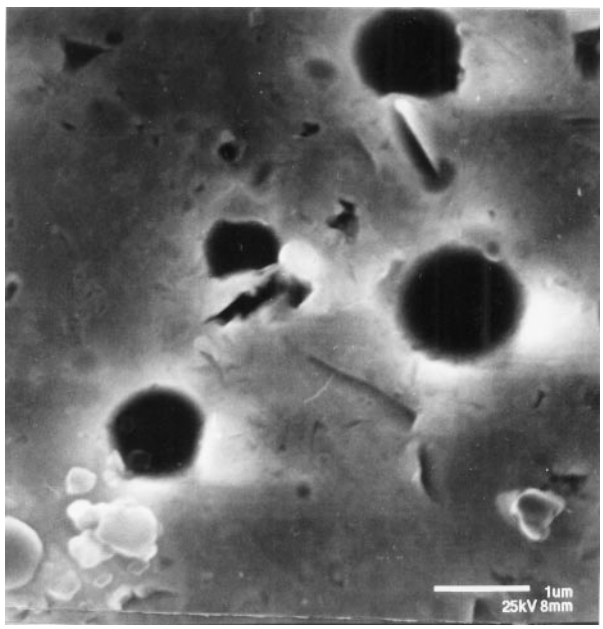

Figure 8 Crater produced by impact of 25 μm spherical particles. Note asymmetric pile up at certain location of the periphery.

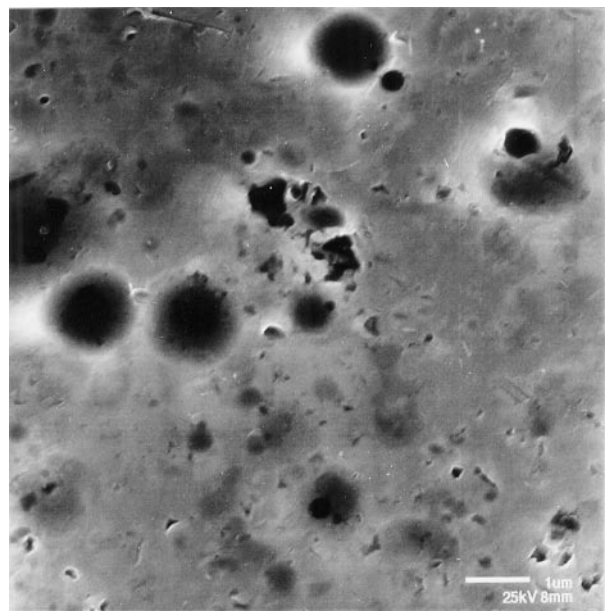

Figure 9 Other craters from randomly selected grain caused by 25 μm spherical particles.

In addition, single crystals (or individual grains in a polycrystalline material) exhibit anisotropy in yield and tensile strength [17–20]. Therefore, asymmetrical pile-up formation at the rim of craters, regardless of particle geometry, could be attributed to the crystallographic orientation of the grain. The dominant deformation mechanism for spherical particles still persists and exhibits identical features to those obtained from angular particles. Anisotropic mechanical properties of the individual grains dominate the impact damage morphology. Determination of crystallographic orientation of individual grains, on which highly directional material flow is observed, would further enhance this statement.

Damage characteristics of indentations created by spherical and angular particles within the same grain observed here in lend support to the proposed deformation mechanism, the resultant, general perspective of deformation features exhibit a similar mechanism, that is, crystallography oriented deformation, is operative.

As already stated at the beginning of the article, these unique observations elucidate the deformation mechanism operating at the impact of small particles

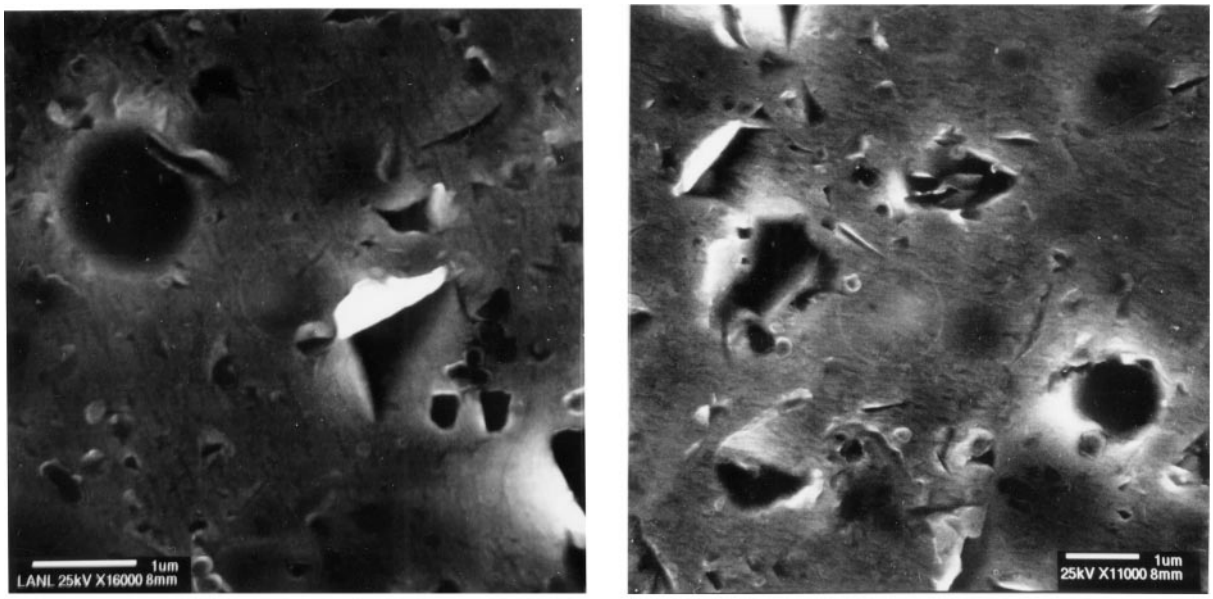

(a) (b)

Figure 10 a and b target surface exposed to the mixture of 25 μm spherical and angular particles. Note the direction of material flow regardless of particle geometry.

to a target surface. With increasing particle size, deformation mechanism and the associated deformation features dramatically change for the same target material having same grain size. This issue is the subject of another article by the same authors [14, 15].

5. Conclusions

1. Rather than the macroscopic mechanical properties of polycrystalline target material, mechanical response of the deforming individual grain seems to determine impact damage mechanism in solid particle erosion caused by small particles.

2. Highly directional chip formation is related to the anisotropic mechanical properties of individual grains.

3. Impact damage morphology and the associated asymmetry varies from grain to grain, thus, crystallographic orientation of that particular grain is an important factor for the present observations.

4. Angularity of the particles appears to have significant contribution to the impact damage morphology in that severity of the damage increases with the increased angularity.

References

1. T. CHRISTMAN and P. G. SHEWMON, *Wear* **54** (1979) 145.
2. G. L. SHELDON and A. KANHERE, *ibid.* **21** (1972) 195.
3. Y. I. OKA, H. OHNOGI, T. HOSOKAWA and M. MATSUMURA, *ibid.* **203/204** (1997) 573.
4. A. V. LEVY, Z. R. SHUI and B. W. WAVY, in Proceeding 7th Conference on Erosion by Liquid and Solid Impact (1987) 51-1, 51-9.
5. A. V. REDDY and G. SUNDARARAJAN, *Metallurgical Transactions A* **18A** (1987) 1043.
6. R. BROWN and J. W. EDINGTON, *Wear* **69** (1981) 369.
7. I. FINNIE, *ibid.* **186/187** (1995) 1.
8. I. M. HUTCHING and A. V. LEVY, *ibid.* **131** (1989) 105.
9. A. BALL, *ibid.* **91** (1983) 201.
10. G. SUNDARARAJAN and R. MANISH, *Tribology International* **30** (1997) 339.
11. K. C. GORETTA, R. C. ARRAYO, C. T. WU and J. L. ROUTBORT, *Wear* **147** (1991) 145.
12. Potter, Industries, DA, Technical Data Sheet, 1997.
13. O. T. INAL, M. BENGISU, B. MORTON and R. RICHMAN, *Review of Scientific Instruments* **66** (1995) 3649.
14. M. DUNDAR and O. T. INAL, *Wear* **224** (1998) 226.
15. M. DUNDAR, Dissertation (1998), New Mexico Institute of Mining and Technology.
16. M. DUNDAR and O. T. INAL, (1998) Submitted for publication.
17. E. SCHMID and W. BOAS, " Plasticity of Crystals" (Chapman Hall, London, 1968).
18. R. W. ARMSTRONG and A. C. RAGHURAM, in "The Science of Hardness Testing and its Research Applications," edited by J. H. Westbrook and H. Conrad (ASM, Metals Park, OH, 1972) p. 174.
19. F. W. DANIELS and C. G. DUNN, *Transactions of the American Society for Metals* **41** (1949) 419.
20. E. R. PETTY, *Journal of the Institute of Metals* (1962-63) 54.

Received 16 September
and accepted 14 December 1999